

# $\alpha,\alpha'$ -Diamino-*p*-tetrafluoroquinodimethane: Stability of One- and Two-Electron Oxidized Species and Fixation of Molecular Oxygen

Alok Mahata, Nicolas Chrysochos, Ivo Krummenacher, Shubhadeep Chandra, Holger Braunschweig,\* Carola Schulzke,\* Biprajit Sarkar,\* Cem B. Yildiz,\* and Anukul Jana\*

Cite This: *J. Org. Chem.* 2021, 86, 10467–10473

Read Online

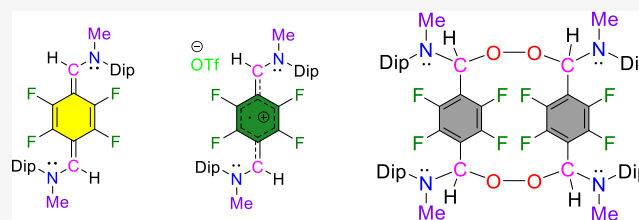
ACCESS |

Metrics & More

Article Recommendations

Supporting Information

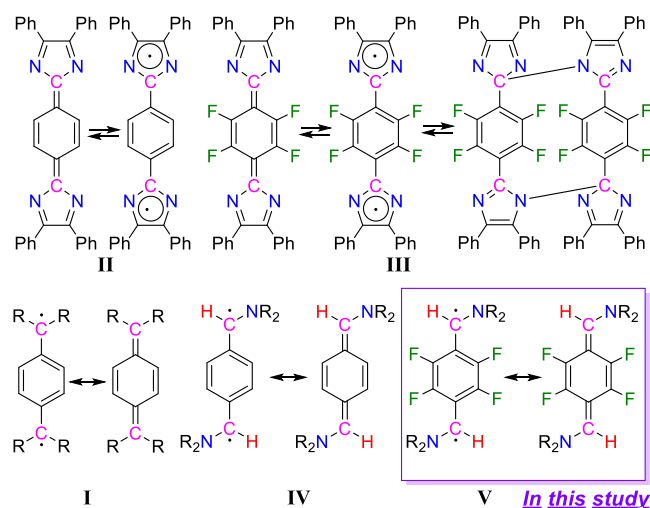
**ABSTRACT:** Herein, we report the synthesis, characterization, and reactivity of  $\alpha,\alpha'$ -diamino-*p*-tetrafluoroquinodimethane, a *p*-tetrafluorophenylene-bridged monosubstituted carbene-based Thiele's hydrocarbon A. The compound exhibits a reversible two-step one-electron oxidation with a marginally stable radical cation state B. The *in situ* formation of the radical cation could be confirmed by electron paramagnetic resonance spectroscopy. Interestingly,  $\alpha,\alpha'$ -diamino-*p*-tetrafluoroquinodimethane fixates atmospheric oxygen to form a 16-membered peroxide-bridged macrocyclic compound C.



## INTRODUCTION

The chemistry of *p*-quinodimethanes I (Scheme 1) is important due to their striking properties and various

### Scheme 1. Chemical Structures of I–V



applications.<sup>1</sup> This class of compounds can have two resonance forms: closed-shell quinoid and open-shell benzenoid. Different substitutions (ENG vs EDG vs EWG) at the  $\alpha$ -positions of I (Scheme 1) are known, and it has been documented that the substituents play an important role in their properties.<sup>2</sup> At the same time, the change of H substituents of the central phenylene ring to F substituents can also influence the properties of these compounds.<sup>3</sup> In general, the effects of introducing F substituents into compounds are well-known in various classes of molecules such as in semiconducting

polymers.<sup>4</sup> In 2004, Abe et al. reported the enhancement of the biradical character by changing the H substituents of the central  $\pi$ -conjugated bridge of II to F (Scheme 1).<sup>5</sup> As a result of this change, compound III undergoes reversible dimerization and this has been structurally characterized (Scheme 1). In recent years, several different carbene end-group-based *p*-quinodimethanes have been reported independently by Roesky et al.,<sup>6</sup> Ghadwal et al.,<sup>7</sup> and our group.<sup>8</sup> Sen et al. reported saturated NHC end-group-based *p*-tetrafluoroquinodimethane.<sup>9</sup> Very recently, we have reported  $\alpha,\alpha'$ -diamino-*p*-quinodimethanes IV (Scheme 1) with three isolable oxidation states: neutral, radical cation, and dication.<sup>10</sup> Compound IV can be considered as a formally monosubstituted carbene<sup>11</sup> end-group-based *p*-quinodimethane derivative.

We became interested in the synthesis of  $\alpha,\alpha'$ -diamino-*p*-tetrafluoroquinodimethane V (Scheme 1). Our study shows that the resulting  $\alpha,\alpha'$ -diamino-*p*-tetrafluoroquinodimethane forms only a marginally stable radical cation state. This is in stark contrast to observations on compound IV and points to the influence of the replacement of H by F of the central *p*-phenylene bridge. Moreover,  $\alpha,\alpha'$ -diamino-*p*-tetrafluoroquinodimethane V can perform the fixation of atmospheric molecular oxygen under ambient conditions, leading to the formation of a 16-membered macrocyclic compound with two peroxide linkages. *p*-Quinodimethane is known to form a peroxide-bridged polymer upon reaction with molecular

Received: May 12, 2021

Published: July 16, 2021

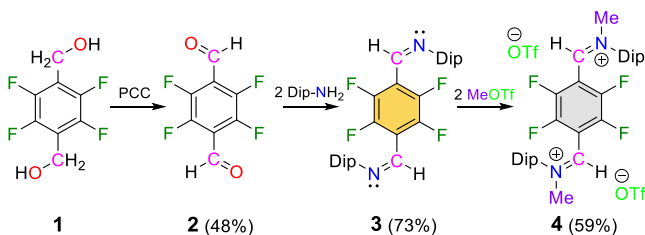


oxygen.<sup>12</sup> However, it is well-known that localized radicals form discrete peroxide compounds upon reaction with molecular oxygen.<sup>13</sup>

## RESULTS AND DISCUSSION

For the synthesis of the targeted  $\alpha,\alpha'$ -diamino-*p*-tetrafluoroquinodimethane, we synthesized the corresponding two-electron oxidized bis-iminium-cation **4** as a synthon<sup>14</sup> as shown in Scheme 2.<sup>15</sup>

**Scheme 2.** Synthesis of **2**, **3**, and **4** (PCC = pyridinium chlorochromate, Dip = 2,6-*i*Pr<sub>2</sub>C<sub>6</sub>H<sub>3</sub>, OTf<sup>-</sup> = trifluoromethanesulfonate)



Compound **4** was characterized by solution-state multinuclear magnetic resonance spectroscopy along with single-crystal X-ray diffraction analysis (Figure 1).

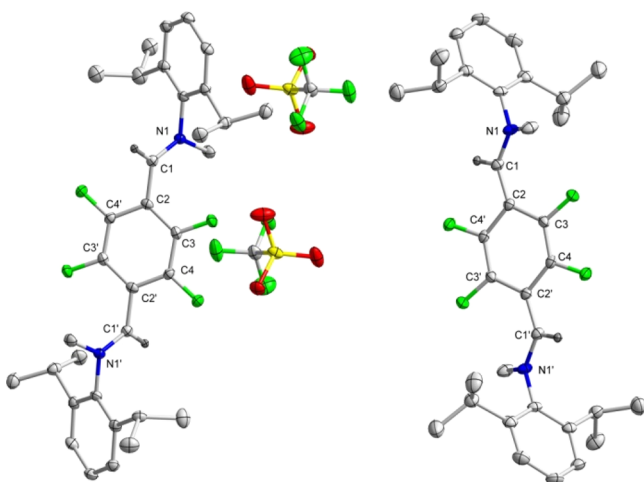


**Figure 1.** Solid-state molecular structures of **4** and **5** with thermal ellipsoids at the 50% probability level. All H atoms except C1-H and C1'-H have been omitted for the sake of clarity. Selected bond lengths (Å) and bond angles (°) for **4**: N1–C1, 1.282(2); C1–C2, 1.463(2); C2–C3, 1.389(2); C3–C4, 1.371(2); N1–C1–C2, 124.94(13). Selected bond lengths (Å) and bond angles (°) for **5**: N1–C1, 1.368(2); C1–C2, 1.377(2); C2–C3, 1.444(2); C3–C4, 1.345(2); N1–C1–C2, 131.21(12).

A cyclic voltammetry study of compound **4** shows that the signals of the cathodic wave were merged into one broad signal at room temperature, while two separate anodic waves were observed (Figure S29).<sup>15</sup> However, when the cyclic voltammogram was recorded at  $-15\text{ }^{\circ}\text{C}$ , two one-electron redox waves with potentials of  $-0.26$  and  $-0.38$  V versus Fc/Fc<sup>+</sup> (Figure 2) were observed.<sup>15</sup> The difference in potential  $\Delta E_{1/2}$  between the two one-electron redox waves is only 0.12 V (in the case of corresponding nonfluorinated compound **5-H**  $\Delta E_{1/2}$  is 0.48 V) (Table 1), and therefore, an exceptionally low comproportion-

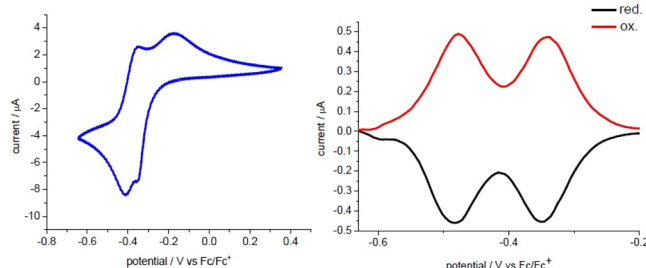


**Figure 2.** Cyclic voltammogram of **4** in CH<sub>3</sub>CN/0.1 M Bu<sub>4</sub>NPF<sub>6</sub> at  $-15\text{ }^{\circ}\text{C}$  (left) and differential pulse voltammograms of **4** in CH<sub>3</sub>CN/0.1 M Bu<sub>4</sub>NPF<sub>6</sub> at room temperature (right).

nation constant  $K_c$  of 220 is found. The low value of  $K_c$  suggests a poor thermodynamic stability of the one-electron reduced species, and a propensity of this molecule to be stable in the even-electron forms. A differential pulse voltammogram (DPV) study confirms the involvement of two reversible one-electron processes in the electrochemical reduction (Figure 2).<sup>15</sup>

Subsequently, the reduction of **4** with elemental Mg at  $-78\text{ }^{\circ}\text{C}$  leads to **5** as a yellow crystalline solid in a 70% yield (Scheme 3). <sup>19</sup>F/<sup>19</sup>F{<sup>1</sup>H} NMR spectra suggest the formation of two isomers: *syn* and *anti* in a 1.3:1 ratio. In the <sup>19</sup>F{<sup>1</sup>H} NMR spectrum, the *syn*-isomer exhibits two singlets at  $-142.5$  and  $-159.6$  ppm, whereas the *anti*-isomer exhibits two doublets at  $-146.8$  and  $-156.2$  ppm with a  $^3J_{(^{19}\text{F},^{19}\text{F})}$  of 15 Hz. This is in contrast to that of nonfluorinated analogue **5-H**, where the *syn* isomer is the minor species with a *syn:anti* isomer ratio of 30:70. This reflects the influence of F substituents on the relative stability of *syn* and *anti* isomers. DFT calculations at the M06-2X-D3/def2-SVP/SCRF=THF (SMD)//BP86-D3/def2-SVP level of theory suggest that the energy of the *syn* isomer is 1.7 kcal mol<sup>-1</sup> lower than that of the *anti* isomer. The trend is the same at the BP86-D3/def2-SVP and M06-2X-D3/def2-TZVP/SCRF=THF (SMD)//BP86-D3/def2-SVP levels of theory.

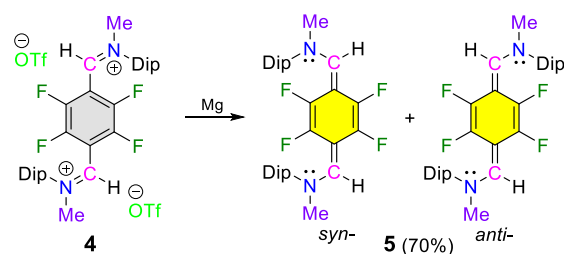
However, the single-crystal X-ray diffraction study of **5** revealed the presence of only the *anti* isomer in the solid state (Figure 1) as in the case of **5-H**. The N1–C1–C2–C3 dihedral angle of **5** is 14.46(14)<sup>o</sup>, whereas for nonfluorinated analogue **5-H**, it is 0.55(12)<sup>o</sup>. This can be attributed to the presence of the F substituents in **5** that provide a steric hindrance and render the H–C–N and central–C<sub>6</sub>F<sub>4</sub> planes non-co-planar. The C1–N1 bond length in **5** is 1.368(2) Å, which is shorter than that of its corresponding nonfluorinated analogue **5-H** [1.376(2) Å].<sup>10</sup> The C1–C2 bond length of **5** is 1.377(2) Å, which is longer than that of **5-H** [1.366(2) Å] but shorter than that of Thiele's hydrocarbon [1.381(3) Å]<sup>16</sup> and CAAC-based Thiele's hydrocarbon [1.381(2) Å].<sup>8a</sup> The bond length alternation (BLA) of the central benzene ring of **5** is 0.099 Å, which is almost similar to those of **5-H** (0.107 Å) and Thiele's hydrocarbon (0.103 Å) (Table 1). Compound **5** is EPR silent in the solid state and in the solution state (toluene) in the temperature range of 20–300 K. This suggests that compound **5** possesses a quinoid singlet ground state with no significant population of the triplet state at room temperature.

Additionally, DFT results depict that the energy of the singlet state of **5** is lower than that of the triplet state by a  $\Delta E_{S-T}$  of  $-23.8$  kcal mol<sup>-1</sup>. The calculated diradical character  $y$  at the CASSCF(2,2)/6-311G(d,p) level of theory for **5** ( $y = 7.7\%$ ) is lower than that of *p*-quinodimethane ( $y = 9.2\%$ ),

Table 1. Comparison of Selected Parameters of 4, 4-H, 5, 5-H, 6, and 6-H

	$E_{1/2}$ (V, first reduction)	$E_{1/2}$ (V, second reduction)	$\lambda_{\max}$ (nm) [ $\epsilon$ ( $L \text{ mol}^{-1} \text{ cm}^{-1}$ )]	C1–N1	C1–C2	C2–C3	C3–C4	BLA	$\angle \text{N1–C1–C2}$	$\angle \text{N1–C1–C2–C3}$
4	−0.26	−0.38	287(18077)	1.282(2)	1.463(2)	1.389(2)	1.371(2)	0.018	124.94(13)	53.92(13)
4-H	−0.53	−1.01	287(38936)	1.287(2)	1.453(2)	1.388(2)	1.371(2)	0.017	129.17(14)	18.63(17)
5			412(31592)	1.368(2)	1.377(2)	1.444(2)	1.345(2)	0.099	131.21(12)	14.46(14)
5-H			403(30673)	1.376(2)	1.366(2)	1.450(2)	1.343(2)	0.107	131.70(12)	00.55(12)
6 <sup>a</sup>			468, 698	1.340	1.424	1.435	1.387	0.048	129.69	28.22
6-H			460(54998), 678(16261)	1.328(3)	1.402(3)	1.427(3)	1.360(3)	0.067	130.80(19)	01.21(20)

<sup>a</sup>The metric parameters of 6 are based on the lowest-energy optimized geometry.

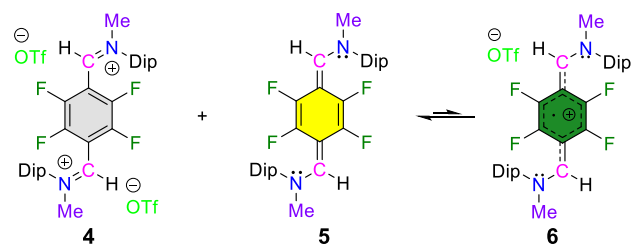
Scheme 3. Synthesis of 5 (Dip = 2,6-*i*Pr<sub>2</sub>C<sub>6</sub>H<sub>3</sub>)

Thiele's hydrocarbon ( $y = 15.7\%$ ), and 5-H ( $y = 8.1\%$ ). For 5, the calculated HOMO–LUMO energy gap ( $\Delta E_{\text{H-L}} = 4.55 \text{ eV}$ ) is determined to be considerably high in comparison to those of *p*-quinodimethane (3.76 eV) and Thiele's hydrocarbon (3.82 eV) but lower than that of 5-H (4.68 eV).<sup>15</sup>

During the synthesis of 5, the appearance was initially deep green before the solution became yellow. This could be an indication of the intermediate formation of one-electron reduced compound 6 with limited stability. Therefore, the reaction of 4 with half an equivalent of Mg or 5 with equivalent amounts of AgOTf does not lead to the isolation of 6. However, its formation could be confirmed by UV–vis spectroscopy and UV–vis spectroelectrochemistry studies.

The comproportionation reaction of 4 and 5 also shows the formation of a deep green colored solution (Scheme 4). The

## Scheme 4. The 1:1 Reaction of 4 and 5



UV–vis spectrum of the reaction mixture suggests the formation of the corresponding radical cation 6 in small amounts (shows the absorbance at 468 and 698 nm) along with mostly unreacted starting compounds 4 and 5 (Figure 3).

Subsequently, UV–vis spectroelectrochemistry studies of compound 4 clearly indicate the formation of 6 (Figure 4). UV–vis spectroelectrochemistry data and the observation of a very small comproportionation constant  $K_c$  are in line with this assumption. The limited stability of 6 is most likely due to the nonachievable planarity between the H–C–N and central–C<sub>6</sub>F<sub>4</sub> planes.<sup>17</sup> This is reflected in the calculated N1–C1–C2–C3 dihedral angle of the lowest-energy optimized geometry of

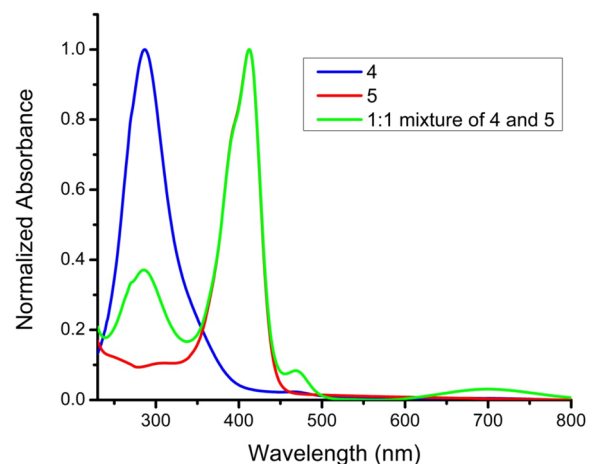


Figure 3. Comparison of UV–vis spectra of compounds 4 and 5 and a 1:1 mixture of 4 and 5 in THF at room temperature.

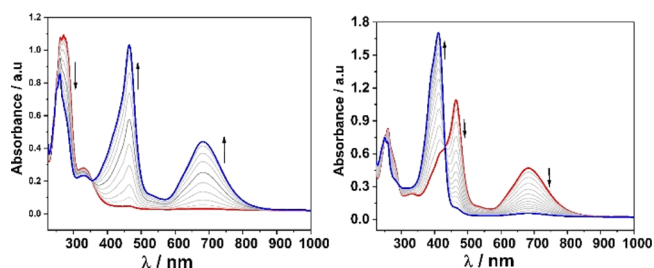
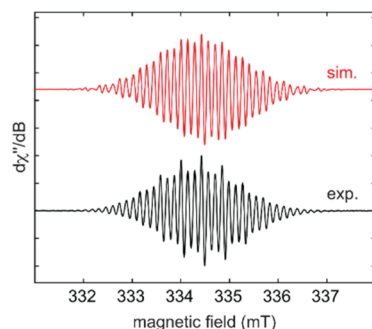


Figure 4. Changes in the UV–vis–near-infrared spectra of 4 during the first reduction (left) and second reduction (right).

radical cation 6 that is 28.22°. This is most likely due to avoiding steric interactions between Dip and F substituents. On the contrary, in the case of the corresponding non-fluorinated radical cation 6-H that was structurally characterized by solid-state single-crystal X-ray diffraction study, the N1–C1–C2–C3 dihedral angle is 1.21(20)° (Table 1). As a result, the spin delocalization of the radical cation over the  $\pi$ -conjugated scaffold is less favorable for 6 than for 6-H. The spin delocalization is the key factor for the formation and subsequent stability of the radical cation. This is directly reflected in the stability of 6 versus 6-H as well as in the separation of  $E_{1/2}$  (first oxidation) and  $E_{1/2}$  (second oxidation).

However, the formation of 6 was observed by solution-state EPR spectroscopy of a 1:1 mixture of 4 and 5 (Figure 5).<sup>15</sup> The best-fit simulation parameters suggest a highly delocalized unpaired electron spin density, with hyperfine couplings to the fluorine, nitrogen, methine, and methyl protons. We have calculated EPR parameters considering all four computational



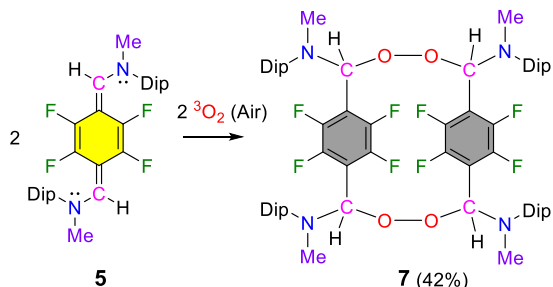
**Figure 5.** Experimental (black) and simulated (red) X-band EPR spectra obtained from a 1:1 mixture of **4** and **5** in THF. Best-fit simulation parameters:  $g_{\text{iso}} = 2.0033$ ,  $a(^{19}\text{F}) = 11.4$  MHz (4F),  $a(^{14}\text{N}) = 11.8$  MHz (2N),  $a(^1\text{H}) = 15.7$  MHz (2H), and  $a(^1\text{H}) = 8.3$  MHz (Me).

minima of radical cation **6** at the BP86/EPR-III level of theory. The EPR parameters  $a(^{19}\text{F})$  in *anti-6* (12.7 MHz in the gas phase and 13.3 MHz in THF) show a close resemblance to the simulated value (11.4 MHz in THF). However, the calculations somewhat overestimate the EPR parameters of  $a(^{14}\text{N})$ ,  $a(^1\text{H})$  of NCH, and  $a(^1\text{H})$  of  $\text{CH}_3$  (Table S9).

Time-dependent density functional theory (TD-DFT) calculations suggest that the experimentally observed band at 412 nm for **5** consists of the HOMO  $\rightarrow$  LUMO (95%) and HOMO  $\rightarrow$  LUMO+4 (5%) transitions. The HOMO is primarily delocalized over the C=C bonds, whereas the LUMO is located in antibonding orbitals over the central C6 ring. The calculations on **4** indicate that the band at 287 nm is mainly (95%) due to the transition from HOMO-5 to LUMO. The observed bands from **6** at 468 and 698 nm can be ascribed to the SOMO $\beta$ -5  $\rightarrow$  LUMO $\beta$ +1 (76%) and SOMO $\alpha$   $\rightarrow$  LUMO $\alpha$  (90%) transitions, respectively.<sup>15</sup>

Despite compound **5** having a closed-shell quinoid ground state, it reacts with atmospheric molecular oxygen under the formation of the entropically disfavored bis-peroxo bridged dimer **7**, a macrocyclic compound with a 16-membered macrocyclic ring (Scheme 5). Under similar reaction

#### Scheme 5. Reaction of **5** with $\text{O}_2$



conditions, **5-H** leads to unidentified compounds. The formation energy of the structure **7** is calculated to be highly exergonic ( $\Delta G = -82.1$  kcal mol<sup>-1</sup>) at the M06-2X-D3/def2-SVP/SCRF=Heptane (SMD)//BP86-D3/def2-SVP level of theory.

The  $^{19}\text{F}\{^1\text{H}\}$  NMR spectrum exhibits two resonances at  $-143.3$  and  $-135.8$  ppm, which suggest the formation of only one isomer. Crystallographic analysis of **7** revealed O–O and O–C bond lengths of 1.477(2) and 1.459(2) Å, respectively, which are close to typical O–O and O–C bond lengths in

reported peroxides (Figure 6).<sup>18</sup> The two  $\text{C}_6\text{F}_4$  planes are parallel to each other with a distance between them of only

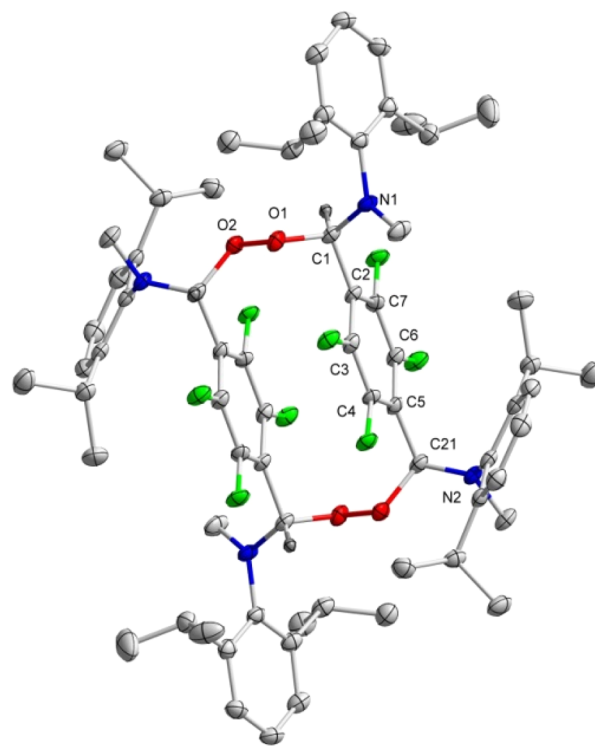


**Figure 6.** Molecular structure of **7** with thermal ellipsoids at the 50% probability level. All H atoms except C1-H, C21-H, C1'-H, and C21'-H have been omitted for the sake of clarity. Selected bond lengths (Å): O1–O2, 1.477(2); O1–C1, 1.459(2); N1–C1, 1.409(3); C1–C2, 1.521(3).

3.19 Å. The solid-state FT-IR spectrum exhibits a stretching vibration frequency at 865 cm<sup>-1</sup> for the O–O peroxide linkage.<sup>19</sup>

In conclusion, we have successfully synthesized and structurally characterized a  $\alpha,\alpha'$ -diamino-*p*-tetrafluoroquinodimethane, which can be considered as a *p*-tetrafluorophenylene-bridged monosubstituted carbene-based Thiele's hydrocarbon. It exhibits three oxidation states: a neutral species, a marginally stable but observable and detectable radical cation, and a dicationic state.  $\alpha,\alpha'$ -Diamino-*p*-tetrafluoroquinodimethane can react with atmospheric molecular oxygen under the formation of a 16-membered doubly peroxide-bridged macrocyclic compound.

## EXPERIMENTAL SECTION

**General Considerations.** All experiments were carried out under an argon atmosphere using standard Schlenk techniques or in a PL-HE-2GB Innovative Technology GloveBox and MBraun Unilab SP GloveBox. Hexane, diethyl ether, THF, and toluene were dried by a PS-MD-5 Innovative Technology solvent purification system. 2,3,5,6-Tetrafluoro-1,4-benzenedimethanol (TCI Chemicals), 2,6-diisopropylaniline (Sigma-Aldrich), magnesium (Sigma-Aldrich), and MeOTf (Sigma-Aldrich) were commercially purchased and used as is. We activated the magnesium before reactions by heating it at a high temperature (using a hot gun at 550 °C) under vacuum for an ~5 min. Benzene-*d*<sub>6</sub> was dried and distilled over potassium under argon. Chloroform-*d*<sub>1</sub> and CD<sub>3</sub>CN were dried and distilled over CaH<sub>2</sub> under argon. NMR spectra were recorded on a BrukerNanoBay 300 MHz NMR spectrometer.  $^1\text{H}$  and  $^{13}\text{C}\{^1\text{H}\}$  NMR spectra were referenced to the peaks of residual protons of the deuterated solvent ( $^1\text{H}$ ) or the

deuterated solvent itself ( $^{13}\text{C}\{^1\text{H}\}$ ).  $^{19}\text{F}\{^1\text{H}\}$  NMR spectra were referenced to external Tol- $\text{CF}_3$ . We have used DEPT90, DEPT135,  $^1\text{H}$ - $^1\text{H}$  COSY, and  $^1\text{H}$ - $^{13}\text{C}\{^1\text{H}\}$  HMQC to assign NMR peaks. Elemental analyses were performed on a PerkinElmer Analyzer 240 instrument. High-resolution mass spectrometry data were obtained from a Thermo Scientific Exactive Plus spectrometer in LIFDI mode for compounds 4 and 5. A Bruker Daltonics micrOTOF-Q instrument was used for electrospray mass spectrometry for the HRMS of compounds 3 and 7. Melting points were determined in closed NMR tubes under a  $\text{N}_2$  atmosphere and are uncorrected. UV-vis spectra were recorded using a Jasco V-670 spectrometer using quartz cells with a path length of 0.1 cm. EPR measurements at X-band (9.38 GHz) were carried out using a Bruker ELEXSYS E580 CW EPR spectrometer equipped with an Oxford Instruments helium cryostat (ESR900) and a MercuryITC temperature controller. The spectral simulations were performed using MATLAB 9.8.0.1323502 (R2020a) and the EasySpin 5.2.28 toolbox.<sup>30</sup> The IR spectrum was recorded on a Nicolet iS5 FTIR spectrometer.

**Synthesis of 2.** A solution of 2,3,5,6-tetrafluoro-1,4-benzenedimethanol 1 (2.1 g, 10 mmol) and PCC (4.74 g, 22 mmol) in 150 mL of dry DCM was refluxed for 2 h using a hot oil bath under a nitrogen atmosphere. After 2 h, the reaction mixture was allowed to cool to room temperature and extracted with DCM and distilled water. The organic part was collected and evaporated to yield solid 2,3,4,5-tetrafluoroterephthaldehyde 2.<sup>21</sup> Without further purification, we proceeded to the next step. Yield: 0.99 g (4.8 mmol, 48%).  $^1\text{H}$  NMR (300 MHz,  $\text{CDCl}_3$ , 298 K):  $\delta$  10.35 (s, 2H, OCH).  $^{13}\text{C}\{^1\text{H}\}$  NMR (75.4 MHz,  $\text{CDCl}_3$ , 298 K):  $\delta$  181.9 (m, 2C, OCH), 146.7 (4C, doublet of multiplets,  $^1J_{\text{F-C}} = 261$  Hz,  $\text{C}_6\text{F}_4\text{-CF}$ ), 118.8 (2C, *ipso*- $\text{C}_6\text{F}_4\text{-C}$ ).  $^{19}\text{F}\{^1\text{H}\}$  NMR (282.4 MHz,  $\text{CDCl}_3$ , 298 K):  $\delta$  -143.7.

**Synthesis of 3.** To a solution of 2,3,4,5-tetrafluoroterephthaldehyde 2 (0.91 g, 4.4 mmol) and *p*-TSA (0.17 g, 0.88 mmol) in 40 mL of methanol was added dropwise a solution of 2,6-diisopropylaniline (1.72 g, 9.68 mmol, in 20 mL of methanol) at room temperature. After completion of the addition, the reaction mixture was stirred for 4 h. After completion of the reaction, a light-yellow precipitate was formed. The resulting precipitate was collected by filtration and washed with 10 mL of methanol to give compound 3. Yield: 1.69 g (3.22 mmol, 73%). Mp: 144–146 °C.  $^1\text{H}$  NMR (300 MHz,  $\text{CDCl}_3$ , 298 K):  $\delta$  8.45 (s, 2H, NCH), 7.23–7.14 (m, 6H, *m*- and *p*-Dip-H), 3.05–2.92 (m, 4H,  $\text{CH}(\text{CH}_3)_2$ ), 1.22 (d,  $J = 6.9$  Hz, 24H,  $\text{CH}(\text{CH}_3)_2$ ).  $^{13}\text{C}\{^1\text{H}\}$  NMR (75.4 MHz,  $\text{CDCl}_3$ , 298 K):  $\delta$  151.9 (2C, NCH), 149.2 (2C, *ipso*-Dip-C), 145.9 (4C, doublet of multiplets,  $^1J_{^{19}\text{F},^{13}\text{C}} = 261$  Hz,  $\text{C}_6\text{F}_4\text{-CF}$ ), 137.1 (4C, Dip-CCH( $\text{CH}_3$ )<sub>2</sub>), 125.3 (2C, *p*-Dip-CH), 123.4 (4C, *m*-Dip-CH), 117.2 (2C, *ipso*- $\text{C}_6\text{F}_4\text{-C}$ ), 28.2 (4C, CCH( $\text{CH}_3$ )<sub>2</sub>), 23.6 (8C,  $\text{CH}(\text{CH}_3)_2$ ).  $^{19}\text{F}\{^1\text{H}\}$  NMR (282.4 MHz,  $\text{CDCl}_3$ , 298 K):  $\delta$  -143.1. Elemental Anal. Calcd for  $\text{C}_{32}\text{H}_{36}\text{F}_4\text{N}_2$ : C, 73.72; H, 6.92; N, 5.34. Found: C, 73.04; H, 6.94; N, 5.45. HRMS (ESI):  $m/z$  [ $\text{M} + \text{H}$ ]<sup>+</sup> calcd for  $\text{C}_{32}\text{H}_{37}\text{F}_4\text{N}_2$  525.2893, found 525.2888.

**Synthesis of 4.** A solution of MeOTf (1.05 g, 0.7 mL, 6.34 mmol, in 15 mL of dry DCM) was added slowly to the solution of 3 (1.51 g, 2.88 mmol, in 40 mL of dry DCM) at -78 °C. After completion of the addition, the reaction mixture was slowly warmed to room temperature and was stirred overnight. The next day, all volatiles were removed by vacuum evaporation and the residue was washed with 50 mL of dry  $\text{Et}_2\text{O}$  to yield 4 as white powder. A saturated solution of 4 in dry DCM at -20 °C yielded suitable single crystals for the X-ray diffraction study after 2 days. Yield: 1.45 g (1.7 mmol, 59%). Mp: 185–187 °C dec.  $^1\text{H}$  NMR (300 MHz,  $\text{CD}_3\text{CN}$ , 298 K):  $\delta$  9.57 (s, 2H, NCH), 7.68 (t,  $J = 7.8$  Hz, 2H, *p*-Dip-H), 7.53 (d,  $J = 7.8$  Hz, 4H, *m*-Dip-H), 4.14 (s, 6H,  $\text{NCH}_3$ ), 2.95–2.81 (m, 4H,  $\text{CH}(\text{CH}_3)_2$ ), 1.37 (d,  $J = 6.9$  Hz, 12H,  $(\text{CH}_3)\text{CH}(\text{CH}_3)$ ), 1.31 (d,  $J = 6.9$  Hz, 12H,  $(\text{CH}_3)\text{CH}(\text{CH}_3)$ ).  $^{13}\text{C}\{^1\text{H}\}$  NMR (75.4 MHz,  $\text{CD}_3\text{CN}$ , 298 K):  $\delta$  170.2 (2C, NCH), 145.4 (4C, doublet of multiplets,  $^1J_{^{19}\text{F},^{13}\text{C}} = 265$  Hz,  $\text{C}_6\text{F}_4\text{-CF}$ ), 142.6 (4C, Dip-CCH( $\text{CH}_3$ )<sub>2</sub>), 141.1 (2C, *ipso*-Dip-C), 133.4 (2C, *p*-Dip-CH), 126.7 (4C, *m*-Dip-CH), 114.7 (2C, *ipso*- $\text{C}_6\text{H}_4\text{-C}$ ), 51.2 (2C,  $\text{NCH}_3$ ), 29.4 (4C,  $\text{CH}(\text{CH}_3)_2$ ), 24.6 (4C,  $\text{CH}(\text{CH}_3)_2$ ), 24.0 (4C, CCH( $\text{CH}_3$ )<sub>2</sub>).  $^{19}\text{F}\{^1\text{H}\}$  NMR (282.4 MHz,  $\text{CD}_3\text{CN}$ , 298 K):  $\delta$  -79.4 (s, 3F,  $\text{CF}_3\text{SO}_3^-$ ), -129.9 (4F,  $\text{C}_6\text{F}_4\text{-CF}$ ). UV-vis

(THF):  $\lambda_{\text{max}}$  ( $\epsilon$ ) = 287 nm (18077 L mol<sup>-1</sup> cm<sup>-1</sup>). ESI-MS: calcd ( $m/z$ ) for  $\text{C}_{34}\text{H}_{42}\text{F}_4\text{N}_2$  554.3279, found 554.3275. Elemental Anal. Calcd for  $\text{C}_{36}\text{H}_{46}\text{F}_6\text{N}_2\text{O}_6\text{S}_2$ : C, 50.70; H, 4.96; N, 3.28. Found: C, 50.04; H, 4.63; N, 3.14.

**Synthesis of 5.** Approximately 30 mL of THF was added to a Schlenk flask containing compound 4 (1 g, 1.17 mmol) and activated Mg (0.042 g, 1.76 mmol) at -78 °C, and then the mixture was stirred for 1 h. Then the reaction mixture was slowly warmed to room temperature and stirred overnight. The color of the reaction solution initially changed to deep green and then finally to light yellow. All volatiles were removed under vacuum, and the resulting residue was extracted using hexane. After the solvent was removed, product 5 was obtained as a yellow crystalline solid. A saturated hexane solution of 5 was kept at -30 °C and gave suitable single crystals for the X-ray diffraction study after 2 days.  $^{19}\text{F}$  and  $^{19}\text{F}\{^1\text{H}\}$  NMR spectra show the formation of *syn* and *anti* isomers in a 1.3:1 ratio. Yield: 455 mg (0.82 mmol, 70%). Mp: 130–132 °C.  $^1\text{H}$  NMR (300 MHz,  $\text{C}_6\text{D}_6$ , 298 K):  $\delta$  7.12 (t,  $J = 7.2$  Hz, 2H, *p*-Dip-H, merged with  $\text{C}_6\text{D}_6$  residual proton signals), 7.00 (d,  $J = 7.8$  Hz, 4H, *m*-Dip-H), 6.40 (s, 2H, NCH), 3.18–3.09 (m, 4H,  $\text{CH}(\text{CH}_3)_2$ ), 3.01–2.95 (m, 6H,  $\text{NCH}_3$ ), 1.10–1.15 (m, 24H,  $(\text{CH}(\text{CH}_3)_2)$ ).  $^{13}\text{C}\{^1\text{H}\}$  NMR (75.4 MHz,  $\text{C}_6\text{D}_6$ , 298 K):  $\delta$  146.9, 146.8, 144.5, 144.4, 142.7, 129.8–129.5 (2C, NCH), 124.7 (*p*-Dip-CH), 124.4 (*m*-Dip-CH), 124.0 (*m*-Dip-CH), 45.0–44.4 (2C,  $\text{NCH}_3$ ), 38.5 (2C,  $\text{NCH}_3$ ), 28.5 (4C,  $\text{CH}(\text{CH}_3)_2$ ), 27.9 (4C,  $\text{CH}(\text{CH}_3)_2$ ), 24.6–24.3 (8C,  $\text{CH}(\text{CH}_3)_2$ ).  $^{19}\text{F}\{^1\text{H}\}$  NMR (282.4 MHz,  $\text{C}_6\text{D}_6$ , 298 K):  $\delta$  -142.5 (s, 2F,  $\text{C}_6\text{F}_4\text{-CF}$ , *syn* isomer), -146.8 (s, 2F,  $\text{C}_6\text{F}_4\text{-CF}$ , *anti* isomer), -156.2 (d,  $^3J_{^{19}\text{F},^{19}\text{F}} = 14$  Hz, 2F,  $\text{C}_6\text{F}_4\text{-CF}$ , *anti* isomer), -159.6 (s, 2F,  $\text{C}_6\text{F}_4\text{-CF}$ , *syn* isomer).  $^{19}\text{F}$  NMR (282.4 MHz,  $\text{C}_6\text{D}_6$ , 298 K):  $\delta$  -142.5 (s, 2F,  $\text{C}_6\text{F}_4\text{-CF}$ , *syn* isomer), -146.8 (d,  $^3J_{^{19}\text{F},^{19}\text{F}} = 14$  Hz, 2F,  $\text{C}_6\text{F}_4\text{-CF}$ , *anti* isomer), -156.2 (d,  $^1J_{^{19}\text{F},^{19}\text{F}} = 14$  Hz, 2F,  $\text{C}_6\text{F}_4\text{-CF}$ , *anti* isomer), -159.6 (d,  $J = 1.7$  Hz, 2F,  $\text{C}_6\text{F}_4\text{-CF}$ , *syn* isomer). UV-vis (THF):  $\lambda_{\text{max}}$  ( $\epsilon$ ) = 412 nm (31592 L mol<sup>-1</sup> cm<sup>-1</sup>). ESI-MS: calcd ( $m/z$ ) for  $\text{C}_{34}\text{H}_{42}\text{F}_4\text{N}_2$  554.3279, found 554.3272. Elemental Anal. Calcd for  $\text{C}_{34}\text{H}_{42}\text{F}_4\text{N}_2$ : C, 73.62; H, 7.63; N, 5.05. Found: C, 73.05; H, 7.32; N, 4.75.

**Observation of 6.** *Method 1.* Approximately 15 mL of THF was added to a 1:1 mixture of 4 (150 mg, 0.2 mmol) and 5 (91 mg, 0.2 mmol) at room temperature, and the mixture stirred for 10 min. The color of the reaction solution turned deep green. The formation of compound 5 was studied by UV-vis spectroscopy of the reaction mixture.

*Method 2.* Approximately 30 mL of THF was added to a Schlenk flask containing compound 4 (0.85 g, 1 mmol) and activated Mg (0.012 g, 0.5 mmol) at -78 °C, and then the mixture was stirred for 1 h. The color of the reaction solution turned deep green. The reaction mixture was slowly warmed to room temperature and stirred for an additional 30 min. The formation of compound 6 was studied by UV-vis spectroscopy of the reaction mixture.

*Method 3.* AgOTf (25 mg, 0.1 mmol) was placed in a 25 mL Schlenk flask. 5 (55 mg, 0.1 mmol) was added under a  $\text{N}_2$  atmosphere. Approximately 15 mL of THF was added to the mixture at -78 °C and stirred for 1 h. The color of the reaction solution turned deep green. The reaction mixture was slowly warmed to room temperature and stirred for an additional 30 min. The formation of compound 6 was studied by UV-vis spectroscopy of the reaction mixture.

**Synthesis of 7.** Approximately 15 mL of hexane was added to a 25 mL Schlenk flask containing 5 (100 mg, 0.18 mmol). The stopper was removed, and the flask shaken for 2 min in the presence of air. The stopper was reinserted, and the flask kept for crystallization. After 2 days, colorless crystals of compound 7 had formed. Yield: 45 mg (0.038 mmol, 42%). Mp: 146–148 °C dec.  $^1\text{H}$  NMR (300 MHz,  $\text{CDCl}_3$ , 298 K):  $\delta$  7.18 (t,  $J = 7.8$  Hz, 4H, Dip-H), 7.10 (d,  $J = 7.8$  Hz, 4H, Dip-H), 6.95 (d,  $J = 7.8$  Hz, 4H, Dip-H), 6.01 (s, 4H, NCH), 3.34–3.19 (m, 4H,  $\text{CH}(\text{CH}_3)_2$ ), 2.78 (s, 12H,  $\text{NCH}_3$ ), 1.26 (d,  $J = 6.9$  Hz, 12H,  $(\text{CH}_3)\text{CH}(\text{CH}_3)$ ), 1.07 (d,  $J = 6.9$  Hz, 24H,  $(\text{CH}_3)\text{CH}(\text{CH}_3)$ ), 0.828 (d,  $J = 6.9$  Hz, 12H,  $(\text{CH}_3)\text{CH}(\text{CH}_3)$ ).  $^{13}\text{C}\{^1\text{H}\}$  NMR (75.4 MHz,  $\text{CDCl}_3$ , 298 K):  $\delta$  149.5, 148.93, 141.9, 127.8 (4C, Dip-CH), 124.2 (4C, Dip-CH), 123.8 (4C, Dip-CH), 117.4 (2C, *ipso*- $\text{C}_6\text{F}_4\text{-C}$ ), 92.2 (2C, NCH), 40.0 (2C,  $\text{NCH}_3$ ), 28.4

(4C, CH(CH<sub>3</sub>)<sub>2</sub>), 28.0 (4C, CH(CH<sub>3</sub>)<sub>2</sub>), 25.8 (4C, CH(CH<sub>3</sub>)<sub>2</sub>), 25.6 (4C, CH(CH<sub>3</sub>)<sub>2</sub>), 23.5 (4C, CH(CH<sub>3</sub>)<sub>2</sub>), 23.1 (4C, CH(CH<sub>3</sub>)<sub>2</sub>). <sup>19</sup>F{<sup>1</sup>H} NMR (282.4 MHz, CDCl<sub>3</sub>, 298 K): δ -143.3 (m, 4F, C<sub>6</sub>F<sub>4</sub>-CF), -135.8 (m, 4F, C<sub>6</sub>F<sub>4</sub>-CF). HRMS (ESI): *m/z* [M + H]<sup>+</sup> calcd for C<sub>68</sub>H<sub>85</sub>F<sub>8</sub>N<sub>4</sub>O<sub>4</sub> 1173.6443, found 1173.6438. Elemental Anal. Calcd for C<sub>68</sub>H<sub>84</sub>F<sub>8</sub>N<sub>4</sub>O<sub>4</sub>: C, 69.60; H, 7.22; N, 4.77. Found: C, 69.51; H, 7.34; N, 4.67.

## ■ ASSOCIATED CONTENT

### Supporting Information

The Supporting Information is available free of charge at <https://pubs.acs.org/doi/10.1021/acs.joc.1c01120>.

Plots of NMR spectra for new compounds and complete details of computational calculations (PDF)

FAIR data, including the primary NMR FID files, for compounds 2, 3, 4, 5, and 7 (ZIP)

## Accession Codes

CCDC 2056087–2056089 contain the supplementary crystallographic data for this paper. These data can be obtained free of charge via [www.ccdc.cam.ac.uk/data\\_request/cif](http://www.ccdc.cam.ac.uk/data_request/cif), or by emailing [data\\_request@ccdc.cam.ac.uk](mailto:data_request@ccdc.cam.ac.uk), or by contacting The Cambridge Crystallographic Data Centre, 12 Union Road, Cambridge CB2 1EZ, UK; fax: +44 1223 336033.

## ■ AUTHOR INFORMATION

### Corresponding Authors

**Holger Braunschweig** – Institute of Inorganic Chemistry and Institute for Sustainable Chemistry and Catalysis with Boron (ICB), Julius-Maximilians-Universität Würzburg, 97074 Würzburg, Germany; [orcid.org/0000-0001-9264-1726](https://orcid.org/0000-0001-9264-1726); Email: [h.braunschweig@uni-wuerzburg.de](mailto:h.braunschweig@uni-wuerzburg.de)

**Carola Schulzke** – Institut für Biochemie, Universität Greifswald, D-17489 Greifswald, Germany; [orcid.org/0000-0002-7530-539X](https://orcid.org/0000-0002-7530-539X); Email: [carola.schulzke@uni-greifswald.de](mailto:carola.schulzke@uni-greifswald.de)

**Biprajit Sarkar** – Universität Stuttgart, Fakultät Chemie, Lehrstuhl für Anorganische Koordinationschemie, Institut für Anorganische Chemie, D-70569 Stuttgart, Germany; [orcid.org/0000-0003-4887-7277](https://orcid.org/0000-0003-4887-7277); Email: [biprajit.sarkar@iac.uni-stuttgart.de](mailto:biprajit.sarkar@iac.uni-stuttgart.de)

**Cem B. Yildiz** – Department of Medicinal and Aromatic Plants, University of Aksaray, 68100 Aksaray, Turkey; [orcid.org/0000-0002-0424-4673](https://orcid.org/0000-0002-0424-4673); Email: [cemburakyildiz@aksaray.edu.tr](mailto:cemburakyildiz@aksaray.edu.tr)

**Anukul Jana** – Tata Institute of Fundamental Research Hyderabad, Hyderabad 500046 Telangana, India; [orcid.org/0000-0002-1657-1321](https://orcid.org/0000-0002-1657-1321); Email: [ajana@tifrh.res.in](mailto:ajana@tifrh.res.in)

### Authors

**Alok Mahata** – Tata Institute of Fundamental Research Hyderabad, Hyderabad 500046 Telangana, India

**Nicolas Chrysochos** – Institut für Biochemie, Universität Greifswald, D-17489 Greifswald, Germany

**Ivo Krummenacher** – Institute of Inorganic Chemistry and Institute for Sustainable Chemistry and Catalysis with Boron (ICB), Julius-Maximilians-Universität Würzburg, 97074 Würzburg, Germany; [orcid.org/0000-0001-9537-1506](https://orcid.org/0000-0001-9537-1506)

**Shubhadeep Chandra** – Universität Stuttgart, Fakultät Chemie, Lehrstuhl für Anorganische Koordinationschemie, Institut für Anorganische Chemie, D-70569 Stuttgart, Germany

Complete contact information is available at: <https://pubs.acs.org/10.1021/acs.joc.1c01120>

## Notes

The authors declare no competing financial interest.

## ■ ACKNOWLEDGMENTS

The authors acknowledge the generous support of the Department of Atomic Energy, Government of India, under Project RTI 4007, SERB (CRG/2019/003415), India, and CSIR [01(2863)/16/EMR-II], India. The numerical calculations reported in this paper were partially performed at TUBITAK ULAKBIM, High Performance and Grid Computing Center (TRUBA resources).

## ■ REFERENCES

- (1) Selected references: (a) Thiele, J.; Balhorn, H. Ueber einen chinoiden Kohlenwasserstoff. *Ber. Dtsch. Chem. Ges.* **1904**, *37*, 1463–1470. (b) Stuyver, T.; Chen, B.; Zeng, T.; Geerlings, P.; De Proft, F.; Hoffmann, R. Do Diradicals Behave Like Radicals? *Chem. Rev.* **2019**, *119*, 11291–11351. (c) Abe, M. Diradicals. *Chem. Rev.* **2013**, *113*, 7011–7088. (d) Imran, M.; Wehrmann, C. M.; Chen, M. S. Open-Shell Effects on Optoelectronic Properties: Antiamipolar Charge Transport and Anti-Kasha Doublet Emission from a N-Substituted Bisphenalenyl. *J. Am. Chem. Soc.* **2020**, *142*, 38–43. (e) Rudebusch, G.; Zafra, J.; Jorner, K.; Fukuda, K.; Marshall, J. L.; Arrechea-Marcos, I.; Espejo, G. L.; Ponce Ortiz, R.; Gómez-García, C. J.; Zakharov, L. N.; Nakano, M.; Ottosson, H.; Casado, J.; Haley, M. M. Diindeno-fusion of an anthracene as a design strategy for stable organic biradicals. *Nat. Chem.* **2016**, *8*, 753–759. (f) Okamoto, Y.; Tanioka, M.; Muranaka, A.; Miyamoto, K.; Aoyama, T.; Ouyang, X.; Kamino, S.; Sawada, D.; Uchiyama, M. Stable Thiele's Hydrocarbon Derivatives Exhibiting Near-Infrared Absorption/Emission and Two-Step Electrochromism. *J. Am. Chem. Soc.* **2018**, *140*, 17857–17861.
- (2) (a) Metzger, R. M. Unimolecular Electrical Rectifiers. *Chem. Rev.* **2003**, *103*, 3803–3834. (b) Zeng, Z.; Shi, X.; Chi, C.; López Navarrete, J. T.; Casado, J.; Wu, J. Pro-aromatic and anti-aromatic  $\pi$ -conjugated molecules: an irresistible wish to be diradicals. *Chem. Soc. Rev.* **2015**, *44*, 6578–6596. (c) Frederickson, C. K.; Rose, B. D.; Haley, M. M. Explorations of the Indenofluorenes and Expanded Quinoidal Analogues. *Acc. Chem. Res.* **2017**, *50*, 977–987.
- (3) (a) Li, J.; Zhang, G.; Holm, D. M.; Jacobs, I. E.; Yin, B.; Stroeve, P.; Mascal, M.; Moulé, A. J. Introducing Solubility Control for Improved Organic P-Type Dopants. *Chem. Mater.* **2015**, *27*, 5765–5774. (b) Sutton, A. L.; Abrahams, B. F.; D'Alessandro, D. M.; Hudson, T. A.; Robson, R.; Usov, P. M. Structural and optical investigations of charge transfer complexes involving the radical anions of TCNQ and F<sub>4</sub>TCNQ. *CrystEngComm* **2016**, *18*, 8906–8914. (c) Senkevich, J. J.; Desu, S. B. Poly(tetrafluoro-*p*-xylylene), a low dielectric constant chemical vapor polymerized polymer. *Appl. Phys. Lett.* **1998**, *72*, 258–260. (d) Chow, S. W.; Loeb, W. E.; White, C. E. Poly( $\alpha,\alpha,\alpha',\alpha'$ -tetrafluoro-*p*-xylylene). *J. Appl. Polym. Sci.* **1969**, *13*, 2325–2332. (e) Wang, J.; Xu, W.; Zhang, J.; Xu, S. Ag Nanoparticles Decorated Small-Sized AgTCNQF<sub>4</sub> Nanorod: Synthesis in Aqueous Solution and Its Photoinduced Charge Transfer Reactions. *J. Phys. Chem. C* **2014**, *118*, 24752–24760.
- (4) (a) Kawashima, K.; Fukuhara, T.; Suda, Y.; Suzuki, Y.; Koganezawa, T.; Yoshida, H.; Ohkita, H.; Osaka, I.; Takimiya, K. Implication of Fluorine Atom on Electronic Properties, Ordering Structures, and Photovoltaic Performance in Naphthobisthiadiazole-Based Semiconducting Polymers. *J. Am. Chem. Soc.* **2016**, *138*, 10265–10275. (b) Aldrich, T. J.; Matta, M.; Zhu, W.; Swick, S. M.; Stern, C. L.; Schatz, G. C.; Facchetti, A.; Melkonyan, F. S.; Marks, T. J. Fluorination Effects on Indacenodithienothiophene Acceptor Packing and Electronic Structure, End-Group Redistribution, and Solar Cell Photovoltaic Response. *J. Am. Chem. Soc.* **2019**, *141*, 3274–

3287. (c) Wolf, J.; Cruciani, F.; El Labban, A.; Beaujuge, P. M. Wide Band-Gap 3,4-Difluorothiophene-Based Polymer with 7% Solar Cell Efficiency: An Alternative to P3HT. *Chem. Mater.* **2015**, *27*, 4184–4187. (d) Yamamoto, K.; Kato, S.; Zajackowska, H.; Marszalek, T.; Blom, P. W. M.; Ie, Y. Effects of fluorine substitution in quinoidal oligothiophenes for use as organic semiconductors. *J. Mater. Chem. C* **2020**, *8*, 3580–3588.

(5) (a) Kikuchi, A.; Iwahori, F.; Abe, J. Definitive Evidence for the Contribution of Biradical Character in a Closed-Shell Molecule, Derivative of 1,4-Bis-(4,5-diphenylimidazol-2-ylidene)cyclohexa-2,5-diene. *J. Am. Chem. Soc.* **2004**, *126*, 6526–6527. (b) Mayer, U.; Baumgärtel, H.; Zimmermann, H. Biradicals, Quinones, and Semiquinones of the Imidazole Series. *Angew. Chem., Int. Ed. Engl.* **1966**, *5*, 311. (c) Sakaino, Y.; Kakisawa, H.; Kusumi, T.; Maeda, K. Structures and chromotropic properties of 1,4-bis(4,5-diphenylimidazol-2-yl)-benzene derivatives. *J. Org. Chem.* **1979**, *44*, 1241–1244.

(6) Mondal, K. C.; Samuel, P. P.; Roesky, H. W.; Niepötter, B.; Herbst-Irmer, R.; Stalke, D.; Ehret, F.; Kaim, W.; Maity, B.; Koley, D. Synthesis and Characterization of a Triphenyl-Substituted Radical and an Unprecedented Formation of a Carbene-Functionalized Quinodimethane. *Chem. - Eur. J.* **2014**, *20*, 9240–9245.

(7) (a) Rottschäfer, D.; Ho, N. K. T.; Neumann, B.; Stammler, H.-G.; van Gastel, M.; Andrada, D. M.; Ghadwal, R. S. N-Heterocyclic Carbene Analogues of Thiele and Chichibabin Hydrocarbons. *Angew. Chem., Int. Ed.* **2018**, *57*, 5838–5842. (b) Rottschäfer, D.; Neumann, B.; Stammler, H.-G.; Andrada, D. M.; Ghadwal, R. S. Kekulé diradicaloids derived from a classical N-heterocyclic carbene. *Chem. Sci.* **2018**, *9*, 4970–4976.

(8) (a) Maiti, A.; Stubbe, J.; Neuman, N. I.; Kalita, P.; Duari, P.; Schulzke, C.; Chandrasekhar, V.; Sarkar, B.; Jana, A. CAAC based Thiele and Schlenk hydrocarbon. *Angew. Chem., Int. Ed.* **2020**, *59*, 6729–6734. (b) Maiti, A.; Chandra, S.; Sarkar, B.; Jana, A. Acyclic diaminocarbene-based Thiele, Chichibabin, and Müller hydrocarbons. *Chem. Sci.* **2020**, *11*, 11827–11833.

(9) Kundu, G.; De, S.; Tothadi, S.; Das, A.; Koley, D.; Sen, S. S. Saturated N-Heterocyclic Carbene Based Thiele's Hydrocarbon with a Tetrafluorophenylene Linker. *Chem. - Eur. J.* **2019**, *25*, 16533–16537.

(10) Mahata, A.; Chandra, S.; Maiti, A.; Rao, D. K.; Yildiz, C. B.; Sarkar, B.; Jana, A.  $\alpha,\alpha'$ -Diamino-*p*-quinodimethanes with Three Stable Oxidation State. *Org. Lett.* **2020**, *22*, 8332–8336.

(11) Nakano, R.; Jazzar, R.; Bertrand, G. A crystalline mono-substituted carbene. *Nat. Chem.* **2018**, *10*, 1196–1200.

(12) Errede, L. A.; Hoyt, J. M. The Chemistry of Xylylenes III. Some Reactions of *p*-Xylylene that Occur by Free Radical Intermediates. *J. Am. Chem. Soc.* **1960**, *82*, 436–439.

(13) (a) Karimi, M. J.; Borthakur, R.; Dorsey, C. L.; Chen, C. H.; Lajeune, S.; Gabbai, F. P. Bifunctional carbenium dications as metal-free catalysts for the reduction of oxygen. *J. Am. Chem. Soc.* **2020**, *142*, 13651–13656. (b) Glidewell, C.; Liles, D. C.; Walton, D. J.; Sheldrick, G. M. Bis(triphenylmethyl) peroxide. *Acta Crystallogr., Sect. B: Struct. Crystallogr. Cryst. Chem.* **1979**, *35*, 500–502. (c) Suzuki, T.; Nishida, J.-I.; Ohkita, M.; Tsuji, T. Preparation, structure, and redox reactions of nine-membered cyclic peroxides: a novel electrochromic system undergoing reversible extrusion and trapping of O<sub>2</sub>. *Angew. Chem., Int. Ed.* **2000**, *39*, 1804–1806.

(14) (a) Mandal, D.; Sobottka, S.; Dolai, R.; Maiti, A.; Dhara, D.; Kalita, P.; Narayanan, R. S.; Chandrasekhar, V.; Sarkar, B.; Jana, A. Direct access to 2-aryl substituted pyrroliniumsalts for carbon centre based radicals without pyrrolidine-2-ylidene alias cyclic(alkyl)-(amino)carbene (CAAC) as a precursor. *Chem. Sci.* **2019**, *10*, 4077–4081. (b) Nayak, M. K.; Stubbe, J.; Neuman, N. I.; Narayanan, R. S.; Maji, S.; Schulzke, C.; Chandrasekhar, V.; Sarkar, B.; Jana, A. *N,N'*-Ethylene-Bridged Bis-2-Aryl-Pyrrolinium Cations to *E*-Diaminoalkenes: Non-Identical Stepwise Reversible Double-Redox Coupled Bond Activation Reactions. *Chem. - Eur. J.* **2020**, *26*, 4425–4431.

(15) See the [Supporting Information](#) for the NMR spectra, UV–vis spectra, X-ray crystallographic details, and details of theoretical calculations.

(16) Montgomery, L. K.; Huffman, J. C.; Jurczak, E. A.; Grendze, M. P. The molecular structures of Thiele's and Chichibabin's hydrocarbons. *J. Am. Chem. Soc.* **1986**, *108*, 6004–6011.

(17) Messelberger, J.; Grünwald, A.; Goodner, S. J.; Zeilinger, F.; Pinter, P.; Miehlisch, M. E.; Heinemann, F. W.; Hansmann, M. M.; Munz, D. Aromaticity and sterics control whether a cationic olefin radical is resistant to disproportionation. *Chem. Sci.* **2020**, *11*, 4138–4149.

(18) (a) Ghereg, D.; Ech-Cherif El Kettani, S.; Lazraq, M.; Ranaivonjatovo, H.; Schoeller, W. W.; Escudié, J.; Gornitzka, H. An Isolable *o*-Quinodimethane and its Fixation of Molecular Oxygen to give an Endoperoxide. *Chem. Commun.* **2009**, 4821–4823. (b) Uchimura, Y.; Takeda, T.; Katoono, R.; Fujiwara, K.; Suzuki, T. New Insights into the Hexaphenylethane Riddle: Formation of an  $\alpha$ , *o*-Dimer. *Angew. Chem., Int. Ed.* **2015**, *54*, 4010–4013.

(19) Vacque, V.; Sombret, B.; Huvenne, J. P.; Legrand, P.; Suc, S. Characterisation of the O-O peroxide bond by vibrational spectroscopy. *Spectrochim. Acta, Part A* **1997**, *53*, 55–66.

(20) Stoll, S.; Schweiger, A. EasySpin, a comprehensive software package for spectral simulation and analysis in EPR. *J. Magn. Reson.* **2006**, *178*, 42–55.

(21) Dolbier, W. R.; Xie, P.; Zhang, L.; Xu, W.; Chang, Y.; Abboud, K. A. Synthesis of Perfluoro[2.2]paracyclophane. *J. Org. Chem.* **2008**, *73*, 2469–2472.